A Disposable DNA Analysis Chip with a Powerless Actuator

Kyungsup Han
Nanyang Technological University (NTU)
Insup Kim
Korea Advanced Institute of Science and Technology (KAIST)
Wei Xuan Chan
National University of Singapore
Sanglae Kim
Korea Advanced Institute of Science and Technology (KAIST)
Jeong-Hwan Kim
Korea Advanced Institute of Science and Technology (KAIST)
Jinhong Noh
Korea Advanced Institute of Science and Technology (KAIST)
Noori Kim
Newcastle University in Singapore
Yong-Jin Yoon (yongjiny@kaist.ac.kr)
Korea Advanced Institute of Science and Technology (KAIST)

Research Article

Keywords: Disposable DNA Analysis, Chip, Powerless Actuator, non-instrumented, single-use, POC DNA analysism, Ebola

Posted Date: January 3rd, 2022

DOI: https://doi.org/10.21203/rs.3.rs-1122713/v1

Abstract

A non-instrumented, single-use, affordable, and fully- yet safely-disposable DNA analysis system for Point Of Care (POC) diagnostic process has been proposed by integrating (1) a hydration-reactive mixture for a portable heating element as a powerless actuator, (2) commercially available optical adhesive films as valves, and (3) an exothermic reaction-based recombinant polymerase amplification (RPA) process for non-instrumented DNA amplification. The operational error tolerance of the adhesive valves was evaluated by gas production and long-lasting ability, and the amplification performance of the RPA device was validated by gel electrophoresis. Finally, a DNA analysis device was fabricated and tested based on a hydration reaction with a DNA extraction microfluidic channel and an exothermic reaction-based RPA device. In the DNA extraction process, dimethyl adipimidate (DMA) solution was used to eliminate some required injection steps from the extraction process. The integrated system's functionality was successfully demonstrated, and the suggested system could become a foundation for the ultimate total solution for POC DNA analysis.

1. Introduction

The need for point-of-care (POC) devices has been urged by the emergence of a novel coronavirus, SARS-CoV-2[1]. Microfluidic Lab-on-a-Chip (LOC) technologies have brought revolutionary changes and development in the POC platforms by providing easy-to-use, cost-effective miniaturised systems with faster analysis time[2–4]. POC systems have led to effective prevention and early detection of diseases which help deplete mortality drastically[5–7].

Typical POC diagnostic devices, dipstick tests have been widely used for tests of pregnancy, influenza, cardiac markers and other infectious diseases[7–10]. This type of POC diagnostic system, however, has limitations to achieve higher accuracy. For enhancing detection accuracy, nucleic acids (DNA and RNA) are widely used as biomarkers to identify specific infectious diseases[11–13]. However, multi-step and complex fluid handling is essentially required for the workflow of molecular diagnostics[10] (sample preparation, target amplification and signal read-out)[7].

A microfluidic LOC system is the most suitable platform for POC diagnostic system. Bio-analytical devices integrated with the microfluidic component can be used for multi-step processes in a miniaturised system with fast analysis time, high sensitivity and specificity[14,15]. Especially, microfluidic components based polymeric materials have many advantages, including low-cost fabrication, duplicability and disposability. In a nucleic acids LOC system, the three main components that determine its cost, performance and practicability are the pumps/actuators, valves, and the process of nucleic acid amplification.

Microfluidic valves are critical driving components in the LOC system besides pumps and mixers[16,17]. Suitable micropumping methods for flow control represent a major technical hurdle in developing microfluidic systems for point-of-care testing (POCT). Passive pumping for LOC systems is essential in

POC systems[18] to avoid the need for cumbersome external equipment (i.e., syringe pumps and pressure pumps), which are still widely seen in microfluidic devices[19,20]. They control fluid flows by opening or closing fluidic passageways and are usually actuated by external power resulting in a bulky and complex design and limitation in POC testing applications. Various microvalves have been introduced based on their actuating principles, such as electrochemical, piezoelectric, magnetic, electromagnetic, pneumatic, thermopneumatic, shape memory alloy, surface acoustic wave[21–28]. Also, various kinds of powerless valves have been suggested for microfluidic devices[29–31], together with the development of the powerless pump. Capillary force, gravitational force and finger pressure have been widely used as actuation sources to transport samples in POC diagnostic systems[3,32–34]. Three representative methods have a common problem: they are hard to control the flow rate of reagents and use precise control required reaction steps.

An original polymerase chain reaction (PCR) process was designed to amplify a portion of DNA, an essential step for nucleic acid analysis: temperature control is crucial for the procedure. Due to the commonplace features of the methods, PCR is evolved far beyond simple target DNA or RNA detection. Fu, Yayun, et al. describes a low-cost and straightforward self-priming compartmentalisation platform for PCR analysis[35]. The critical element of the platform is the degassed PDMS pump aligned with the outlet port of the chip. It creates the negative pressure in the channel, which automatically derives the sample and oil into a microchamber for self-partition. Therefore, the platform doesn't require an external component that needs power for pumping. Salman, Abbas, et al. report a PCR microfluidic device by integrating three systems: microfluidic PCR chip, thermal cycler, and fluorescence detector[36]. The thin microfluidic layer of the chip facilitates rapid temperature change, allowing fast cycling times. In addition, the device incorporated with photodetector enables further analysis to monitor the PCR progress. But, both devices are not suitable for the POC diagnostic assays due to time demanding and complex external components that need power, respectively.

In addition, nucleic acid testings such as the reverse transcription-polymerase chain reaction (RT-PCR) have become the most reliable method for COVID-19 detection due to their accuracy and sensitiveness to viral genomes recognised as a gold standard by WHO for virus detection technique. Heating elements, however, is not avoidable due to the thermal cycling process of the PCR. Thus, the method heavily depends on the equipment, well-trained staff, and equipped laboratories[37,38].

Unlike conventional PCR, isothermal amplification methods enable the amplification of DNA at one constant temperature. Loop-mediated isothermal amplification (LAMP), recombinant polymerase amplification (RPA), rolling circle amplification (RCA), and helicase dependent amplification (HDA) employ the isothermal method. They have been used for DNA-based POC diagnostic applications[39–44]. The RPA is one of the popular isothermal methods used in POC testing. Its isothermal amplification overcomes shortcomings in temperature control of PCR based tests while providing good sensitivity, low-cost, and fast detection with simple instruments such as paper-based microfluidic devices. It can achieve 10^9–10^{11} fold amplification of target DNA at the optimum temperature around 37–42 ∘C[45]. Although the

RPA method would give more errors and contamination, the reverse-transcription RPA (RT-RPA) was successfully used as an isothermal alternative to RT-PCR for viral disease detection such as Ebola[46].

Researchers have made enormous efforts to develop non-instrumented nucleic acid amplification devices with various isothermal amplification methods to realise equipment-free POC diagnostic systems. Liu et al. developed a self-heating cartridge and maintained a temperature within ±3°C while Huang et al. managed to keep the temperature within ±2°C [47,48]. We believe the non-instrumented RPA device is the most suitable isothermal amplification method for POC applications due to the low operating temperature and less time. Therefore, it is worthy of designing a simple powerless controllable pump with a microvalve and non-instrumented RPA device.

This paper presents a non-instrumented DNA analysis system development that enables total analysis of DNA biomarkers from sample to results within 1 hour. This proof-of-concept study employs 1) a self-powered actuator (or pump) based on a hydration reaction and as a valve; the gas flow is controlled by attaching or detaching a cover film on the microchannels' holes (inlets and outlets). Then 2) an exothermal RPA that amplifies DNA with self-powered heating. We evaluated the performance of these components individually and demonstrated the integrated non-instrumented DNA analysis system.

2. Material And Methods

2.1 Material and Selection of the powder mixture for Hydration reaction based powerless pump and valve

Distilled (DI) water and phosphate-buffered saline (1X PBS) were purchased from Invitrogen (Carlsbad, CA). 3-aminopropyltriethoxysilane (APTES), bovine serum albumin (BSA), dimethyl adipimidate (DMA), sodium bicarbonate, agarose, ethidium bromide (EtBr) were purchased from Sigma-Aldrich (St. Louis, MO, USA). Lysis buffer (AL buffer and proteinase K) was purchased from Qiagen (Hilden, Germany). A portable heating element (powder mixture) was purchased from Outing (Seoul, Korea). Rehydration buffer, dried enzyme pellets and magnesium acetate (MgAc) were purchased from TwistDX (Cambridge, UK). Other chemicals were analytical reagent grade and were used as received. All samples and buffers were prepared using DI water and PBS.

A commercially available optical adhesive film (MicroAmp™, Thermo Fisher Scientific) was utilised as a valve; manually detaching/attaching the piece on chambers acted as open/close valves to control the flow direction. The idea is creative, affordable, straightforward, yet practical for any general microfluidic system design.

The performance of powerless pumps or actuators is evaluated by how easy the flow rate is, how uniform the flow rate is, and how long the operation lasts. For hydration reaction-based, gas-driven pumps, the composition of the powder mixture, amount of powder and amount of water would directly affect the production rate, duration of gas, operating flow rate, and time of the pumps. In this work, we choose a

specific powder mixture that is used as a portable heating element for ready-to-eat products, and it is composed of aluminium (Al; 47%), calcium hydroxide (CaO; 30%), calcium carbonate ($CaCO_3$; 11%), sodium carbonate (Na_2CO_3; 10%) and sodium hydroxide (NaOH; 2%). The mixture of CaO and Al possibly produces heated gases by reacting with water. CaCO3, Na2CO3 and NaOH play a dominant role during the hydration reaction to increase reaction (operating) time. The same mixture is used for both the hydration reaction and exothermal RPA.

2.2 Design and Fabrication of a non-instrumented gas-driven microfluidic system

Metal alloy particles can produce heated gases by reacting with water. The produced gases are potentially used as not only a heat source but also an actuation source. The well-designed composition can make precisely controlled and long-lasting production of gases of metal alloy mixture with other chemical ingredients, and it provides a high-performance powerless micropump. In addition, the gas flow can be controlled by attaching cover films to or detaching cover films from holes of a microchannel (inlet or outlet) for the switching of on-off condition and flow direction.

Figure 1 represents the schematic diagram of the working principle for a hydration reaction-based powerless actuator. Fig. i) and ii) are oversimplified a microchannel to show the basic operational concept for a non-instrumented gas-driven microfluidic system. At the beginning of actuator operation, cover films are detached from the inlet of a microchannel sequentially. Then, water is dropped onto the powder mixture for the hydration reaction using a micro-pipette (i). With the hydration reaction, hydrogen gas is immediately formed. By attaching new cover film onto the inlet hole, the formed hydrogen gas within the limited space of the microchannel pushes reagents along a microchannel to an outlet (ii).

Based on the principle, we design a powerless gas-driven microfluidic device, as shown in Fig. 1. The powder mixture is put in a deep container located at the top end of the microchannel. Before covering the upper layer of a microchannel, we would place reagents in segmented positions of the microchannel with enough clearances according to the reaction sequence. The chemical treated or receptor immobilised part is attached to the opened region of a reaction zone in the microchannel to perform various bio-analysis processes after covering the upper layer. At the last step for the preparation of the microfluidic device, a hole located in the next above the powder mixture is covered with a cover film to prevent pre-reaction of powder mixed with water in the air.

2.3 Development of Exothermic reaction-based recombinant polymerase amplification (RPA) device

The RPA method is one of the isothermal amplification methods; especially, it is performed at relatively low temperatures (37 ~ 42°C) during a shorter process time (25 ~ 35 min) without a thermal cycler. In the experiment, the specific composition of powder mixture in the previous section was used as the solute of exothermic reaction for the heat-up process in the RPA method and water was carried with a Whatman filter paper (Sigma-Aldrich, USA) to the powder container. The RPA device consists of two main parts; the

upper reaction chamber and lower container parts, as shown in Fig. 5(a). All layers of the RPA device were fabricated by CO_2 laser cutting/engraving method using PMMA sheets and assembled by attaching double-sided tapes between layers. The container part includes a container layer with two large holes for a powder container (width: 20 mm, length: 20 mm and height: 3 mm) and a water container (10 mm × 20 mm × 3 mm) and a base layer with an engraved groove for a filter paper. In the reaction chamber part, two floated reaction chambers and a wide hole for the water container were deeply engraved and cut through on a reaction chamber layer, respectively. The layer was covered with a thin top layer cut through with four hoes for a gas vent, two reaction chambers and a water container.

2.4 Design and Fabrication of a Disposable DNA Analysis Chip with a Powerless Actuator

We designed an integrated system that can perform DNA extraction, amplification and read-out without any additional instruments using the powerless hydration reaction-based gas-driven pump and the non-instrumented exothermic reaction-based RPA device. The integrated system, non-instrumented DNA analytical system, consists of four main components: i) reagent reservoir, ii) DNA extraction, iii) DNA amplification & detection and iv) container components, as shown in Fig. 2. First, the reagent reservoir component was designed as an elliptical capsule shape of 9 reservoirs (8 reservoirs with 40 µl volume and a reservoir with 30 µl volume) connected in a line for the storage and separation of reagents depending on their purposes. In addition, the air in empty reservoirs acts as spacers between neighbouring reagents to prevent mixing with each other in the sequential injection process. Second, to perform the DNA extraction process (e.g. lysing, washing, elution steps), we designed 4 mixing channels with a spiral shape (1 mm width) and a long binding channel with a meandering shape (1 mm width). In addition, one end outlet of the binding channel was connected with a channel toward a waste container, and the other outlet was connected with a broken channel near reaction chambers. Third, the waste channel and the broken channel were engraved on the top of a reaction chamber layer. As represented in the previous section, three floated reaction chambers with each 60 µl volume for RPA were deeply engraved from the top of the reaction chamber layer. Lastly, a container of powder for an exothermic reaction, a container of water, and a container of powder for hydration reaction with 6 × 6 mm^2 circular areas were designed as the container components.

All of the designed layers with double-sided tapes were cut or engraved by a CO_2 laser machine. From the bottom side, a base layer, a container layer and a reaction chamber layer were fabricated and assembled using 3 mm thickness of PMMA sheets and 0.1 mm thickness of double-sided tapes, respectively. Then, the reaction chamber layer was covered with a double-sided tape and 0.5 mm thickness of a PMMA sheet. For the reagent reservoir component, 1 mm thickness of a PMMA sheet was cut, and it was attached to the cover layer of the reaction chamber with a double-sided tape. To connect the reagent reservoir layer and the DNA extraction layer, an intermediate layer was fabricated using 0.5 mm thickness of a PMMA sheet and attached between the layers with double-sided tapes. On the top of the integrated system, 50 × 24 mm^2 sized glass, functionalised with an amine group, was attached. In addition, four different designs of detachable channels and covers were cut by CO_2 laser cutting/engraving machine

using optical adhesive films (Invitrogen, USA) (Fig. 2(v)). Finally, the whole system was assembled; double-sided tapes were attached between parts and four detachable channels and covered onto their proper positions.

2.5 Analysis process of DNA from urine sample using the disposable DNA analysis chip with a powerless actuator

The DNA analysis process is started from DNA extraction, and it is ended with the detection of amplified target DNA through DNA amplification. To obtain high-purity DNA, binding DNA extracted from cells using DMA[49] and washing the unbound DNA and other molecules with PBS are necessary for the DNA extraction step. One of the strengths of using DMA as a DNA binding agent is that DMA solution can be mixed with a lysis buffer without inhibition; thus, the solutions can be stored together in a reservoir. As mentioned in the previous section, all reagents used for the DNA analysis are inserted into reservoirs and reaction chambers according to reaction sequences in the fabrication step. Firstly, we placed 11 μl of lysis buffer (10 μl of AL buffer with 1 μl of proteinase K) and 20 μl of 25 mg/ml DMA solution for cell lysis and pre-modification of extracted DNA in the first reservoir of 9 reservoirs near the outlet of a reagent reservoir channel (green-coloured dye). Secondly, we separately placed 120 μl of PBS in fourth, fifth and sixth reagent reservoirs (each 40 μl of PBS) for the washing step of the DNA extraction (blue-coloured dye). Thirdly, we inserted 30 μl of 10 mM sodium bicarbonate (pH 10.6 elution buffer) in the ninth reagent reservoir for the elution of bound DNA (red-coloured dye). Fourthly, 36.8 μl of RPA master mixes used in the test of non-instrumented RPA devices without adding templates (DNA and DI water) were separately inserted into three reaction chambers and 13.2 μl of DI water was only added to the uppermost reaction chamber as a negative control. Lastly, the reaction chambers were covered with an optical adhesive film.

Bi-functional imidoesters of DMA reversibly-covalently bind amine groups on the functionalised surface and the sticky ends of the fragmented DNA. Therefore, we modified the glass surface with amine groups using APTES, a well-known silane-coupling agent and covered a binding channel by the glass. Briefly, the APTES treatment was performed as followed sequences; i) oxygen plasma was used to activate silanol groups on a slide glass using NT-2 plasma cleaning system (Anatech Ltd., CA), ii) the activated glass was immersed with 2% APTES solution in 95% ethanol for 2 hours, iii) the glass was washed with ethanol and DI water for 5 min in three times and dried with a nitrogen stream and iv) finally, curing of the surface was carried out in a convection oven (Memmert, Frankfurt, Germany) at 120°C for 15 min.

3. Results

3.1 Pump validation: Gas producibility and its longlasting ability

As mentioned above, the working principle of a hydration reaction-based powerless actuator is formed gas. The cover film from the inlet of a microchannel is detached. And water is injected into the container of the powder mixture. The inlet hole is again covered by attaching a cover film to transport pre-inserted

reagents to a reaction zone in the microchannel. The pre-inserted reagents with trapped air between reagents would be sequentially flowed and passed away the reaction zone with specific reactions corresponded to treated chemical or immobilised receptors. If needed, wastes and test samples can be separated by blocking or opening outlets with cover films in this process.

With the fixed composition of the powder, the flow rates of reagents can be changed by different amounts of powder or water. In hydration reaction, variations of powder amount are more effective in changing the flow rates than water amount. Therefore, we used different amounts of the powder and 100 µl of water for hydration reaction to demonstrate corresponding flow rates in a simple straight channel (Fig. 3(a)). Test devices were fabricated by a CO_2 laser cutting/engraving machine (Universal laser systems, AZ, USA) using PMMA sheets. A test device consists of an upper cover layer engraved with a millimeter ruler and has three sets of inlets and outlets for three microchannels. This channel layer includes three microchannels designed with 1 x 1 x 25 mm^3 (width x height x length) of dimension and three reagent reservoirs with ellipse shapes for each channel. This lower layer includes an 8 mm diameter of circular cylinder-shaped container for powder mixture, a plat lower cover layer. While the assembling process, 20 µl of green coloured dyes were placed on reagent reservoirs before attaching the upper cover layer.

In order to test the effect of solute amount difference in hydration reaction, we separately put 1, 5 and 10 mg of the powder into inlets of three microchannels in a test device and put 30, 50 and 100 mg of the powder into another test device. Then, hydration reactions were started by injecting 100 µl of water into powder containers and covering inlet holes with cover film and formed gases pushed in dyes through channels to outlets of microchannels. A digital camera recorded the flow motion. The velocity of fluid was obtained using elapsed time for 1 mm movement from the recorded video. Flow rates of fluid were calculated using the velocities and the cross-section area of microchannels. The flow rates based on the experiment shown in Fig. 3(a) were plotted according to the amounts of the powder used for hydration reactions shown in Fig. 3(b). From the graph, results showed that a more significant amount of the powder generates higher flow rates. In addition, the flow rates can be easily controlled with the proper amount of the powder depending on the purposes (mixing, binding or sorting) of the applications for a relatively short length of a microchannel required applications (less than 25 mm).

To use the gas-driven pump for multi-step reactions, flow rate uniformity and long-lasting ability need to be investigated. For the investigation, we designed and fabricated a 1 m length of the microchannel and chose 10 mg of the powder to assume that a lower amount of the powder has a relatively high uniformity of flow rates (Fig. 3(c)). In the same way, 10 mg of the powder was placed in the powder container, and it was activated by 100 µl of water after covering an inlet hole with a cover film. The flow motion was recorded with 1 min of the time interval for 2 hours, and the velocity of fluid was obtained via flow distance per min from the recorded video. Then, flow rates of fluid were calculated and plotted with time, as shown in Fig. 3(d). In the figure, the measured flow rates show that the gas-forming process is maintained by hydration reaction between the tiny amount of the powder (10 mg) and small water drop (100 µl) with a narrow range of flow rates (4 ~ 8 µl/min) for over 2 hours except for 10 min from the

initial reaction. In the particular application that needs to avoid rapidly changing region from 0 to 10 min, we can cover an inlet hole with a cover film at 10 minutes after putting water into the powder container.

3.2 Valve validation: Operational error tolerance

Here we validate the valve design to: (1) allow tolerance for manual handling error and (2) reduce wastage of eluted DNA solution. In a long channel, the hydration reaction (Fig. 4(a)) causes the solution to move to the junction (Fig. 4(b)). At the channel junction after the film cover is removed (Fig. 4(c)) the ratio of solution wastage is 50% (due to equal fluidic resistance) or less. In the event, when the operator erroneously removed the film cover slightly later (when some solution has passed the junction), the ratio of solution flow toward the waster chamber would be lesser. Only 17% of solution flow towards the waste chamber after the film cover was removed in the test. During filling the chamber (Fig. 4(d) to (e)), a ratio of solution wastage is measured to be 11%, lower than when flowing towards the reaction chamber due to the larger dimension of the chamber. The total loss of solution during this period (from Fig. 4(c) to (e)) is 14%. It is possible to reduce the ratio of solution wastage by designing the channel towards the reaction chamber to be shorter but with a larger cross-sectional area (See Fig. 4 (f)). Also, when the reaction chamber is filled up, the remaining fluids flow to waste due to pressure-equalizing (Fig. 4(e), (f)). If enough distance is implemented between reaction and waste solutions, the reaction and waste solutions can be separated naturally.

To counter this loss, it is advisable to include more sodium bicarbonate than the reaction chamber size. Moreover, the design of the valve enables the eluted DNA solution to completely clear into the waste channel once the reaction chamber is filled and prevent overflowing (Fig. 4(d) and (e)) due to the presence of fluidic gravitational pressure and surface tension.

Therefore, the film valve design is a suitable low-cost valve by compromising some losses in the eluted DNA solution.

3.3 RPA device validation : The RPA of nucleic acids with Exothermic reaction-based recombinant polymerase amplification (RPA) device

We developed the exothermic reaction-based recombinant polymerase amplification (RPA) device, and its performance was evaluated. In the exothermic reaction, paper width and powder amount are key factors to achieve the desired temperature and duration of the heat-up process. Accordingly, temperature variations in time were plotted with different amount powders (0.4 and 0.5 g) and different paper widths (3 and 5 mm), as shown in Fig. 5(b). We inserted a digital probe thermometer with a timer (Oneida, USA) into a reaction chamber during the heat-up process and read temperatures from the thermometer per minute for the temperature measurements. In the experiments, the temperature increment is started at 10 min after adding 500 µl of water into the water container of the RPA device and the maximum temperature and overtime of exothermic reaction are varied with different experimental conditions (pale green, pale blue and pale red lines). Based on the results, we realised that the maximum temperature and the reaction over time could be controlled by the width of filter paper (i.e. flow rate of water) and the ratio of the total amount with the flow rate. Consequently, for the RPA method (37 ~ 42°C for 25 ~ 35 min), we

chose 0.5 g of powder and 3 mm width of filter paper, which attains a temperature variation of ±0.5°C for more than 70 mins, comparable with Liu et al.'s[47] and Huang et al.'s[48] works (±3°C and ±2°C respectively).

To confirm the device's performance, RPA of nucleic acids was carried out with human genomic DNA using the reagents and protocols described in the TwistAmp Basic kit (TwistDX, UK). The optimised protocol is as follows; i) 29.5 µl of rehydration buffer, each 2.4 µl of 10 mM forward and reverse primers (forward:5'-GCA GCA TGT CAA GAT CAC AGA TTT TGG GCT and reverse:5'-CAT GTG TTA AAC AAT ACA GCT AGT GGG AAG GCA, 240 bp), 10.7 µl of distilled (DI) water and 2.5 µl of 50 ng/µl human genomic DNA for a test sample or 2.5 µl of nuclease-free water were mixed in 200 ml tubes, and the mixtures were vortexed. Two of 47.5 µl reaction mixtures were mixed with dried enzyme pellets which include dNTPs, adenosine59-triphosphate, phosphor-creatine, creatine kinase, and components of the proteins gp32 (single-stranded DNA binding protein), uvsX (recombinase), and the uvsY (recombinase load factor). To initiate the reactions, 2.5 µl of magnesium acetate (MgAc) was added to each tube. Each 50 µl of the final reaction mixture was separately put into reaction chambers. Finally, reaction chambers were covered with cover films, and reaction mixtures were incubated for 40 min after adding 500 µl of water to a water container (Fig. 5(c)).

The RPA amplicons were visualised by electrophoresis technique using 1% agarose gel with 1.5 µl of ethidium bromide (EtBr). Fig. 5(d) shows the electropherogram result of stained RPA amplicons with EtBr onto agarose matrix according to different sized molecules; three vertical lines indicate DNA ladder (M), amplified test sample (T) and no DNA template (N). For T and N lines, band intensities in the position of the red box directly represent the quantity of *EGFR* genes in RPA amplicons. Therefore, through the dark band in the T line, unlike the N line, we could realise that the RPA of nucleic acids is successfully performed with our RPA device.

3.4 Performance of Disposable DNA Analysis Chip with a Powerless Actuator : DNA analysis

The performance of the developed disposable DNA analysis chip with a powerless actuator was validated in this section. Fig. 6 represents the DNA analysis process in the whole system using coloured dyes. At the beginning of the process, urine sample was applied as followed order (a); i) an optical adhesive film was detached from the holes above the powder container and the first reagent reservoir, ii) 10 µl of the test sample was introduced to the first reagent reservoir using 10 µl of a disposable pipette, iii) 100 µl of DI water was added to the powder container using 100 µl of a disposable pipette and iv) the holes were again covered with an optical adhesive film at 10 min after injecting DI water. As a result, hydrogen gas was formed by the hydration reaction, and the gas started to push reagents in sequence from the mixture of urine sample, lysis buffer and DMA (green-coloured dye) to elution buffer (red-coloured dye) (Fig. 6(b)). In the spiral channels, the cell lysis and binding of DMA with extracted DNA simultaneously occurred. While the mixture was passed through a long meandering channel, the DNA/DMA complexes were captured by the amine group of APTES treated slide glass. According to the

sequential flow, PBS (blue-coloured dye) was secondly flowed through the long meandering channel to wash away non-specific and unbound molecules. In a microchannel with multi-outlets, the flow directions of fluids can be easily controlled by adjusting hydrodynamic resistances ($R = 12\mu l/wh^3$) among microchannels. In this work, to separately guide waste fluids and extracted DNA fluids, we designed two microchannels with different lengths to make the hydrodynamic resistance difference.

In addition, by blocking reaction chambers (i.e. outlets of the relatively shorter channel), we made to flow two solutions (green and blue-coloured dyes) toward a waste container, as shown in Fig. 6 (b-iii). For the next step, to collect extracted DNA, we detached an optical adhesive film from the reaction chambers when the waste fluid was passed entirely through the meandering channel. An elution buffer flows to the reaction chambers due to the high hydrodynamic resistance and hydraulic head of the waste fluid. The chambers have relatively lower pressure through a meandering channel with eluted DNA by breaking the covalent bonds of amine groups between DNA and APTES, as shown in Fig. 6(c). During the process, we observed that the eluted DNA fluid was evenly split into two reaction chambers by the same pressure drop from a junction to outlets of the chambers (Fig. 6(c-ii ~ iv)). Fig. 6(d) shows the operation process of RPA in the system chip. To minimise thermal losses via air in microchannels, a short bridge-channel made by optical adhesive films was detached from the reaction chambers (Fig. 6(d-i)). And a slide glass with 22 × 22 mm^2 areas was again attached to the chambers with double-sided tape (Fig. 6(d-ii)). Finally, by adding 500 µl of water to a water container using a disposable pipette, the exothermic reaction of the powder was started (Fig. 6(d-iii)) and DNA was incubated with RPA reagents for 40 min to amplify extracted DNA (Fig. 6(d-iv)).

4 Conclusion

Various concepts of microfluidic-based POC diagnostic assays and the LOC technologies have been reviewed and refined in this study. The development of a simple, rapid, and low-cost device for quantitative nucleic acid detection is crucial for point-of-care (POC) diagnostic; simplification of the platform's power source and external components are the key to success.

We have developed an innovative yet straightforward system based on a hydration reaction. The hydrogen gas is generated by the hydration reaction of powder with water and expanded to push in reagents through the reaction zone toward the microchannel outlet. A cover film controls the gas flow by attaching and detaching onto/from the microchannel holes. Finally, we have optimised flow conditions for DNA total analysis and demonstrated an exothermic reaction-based non-instrumented RPA device to prove our concept study. The chip is a fully disposable device that can perform DNA amplification via self-powered heating to be adopted in the POC diagnostic process. Various amplified target DNA detection methods can be considered based on objectives and environments for DNA analysis validation. We believe that our system would provide compatibility with any detection methods and enhance convenience and portability.

Declarations

Acknowledgement

This work was supported by the Korea Institute of Energy Technology Evaluation and Planning(KETEP) and the Ministry of Trade, Industry & Energy(MOTIE) of the Republic of Korea (No. 20194030202360) and the National Research Foundation of Korea(NRF) grant funded by the Korea government(MSIT) (No. 2020R1A2C1011859)

Author Contributions

K.H. and I.K. are co-first authors. K.H. and I.K. conceived the study and performed the experiments, interpreted the data, and wrote the main manuscript text. W.C., S.K., J.-H.K., and J.N. provided inspiring suggestions for improvement and prepared figures. N.K. interpreted the data and reviewed the manuscript. Y.-J.Y. conceived and supervised the project. Y.-J.Y. is the primary corresponding author and N.K. is also a co-corresponding author. All authors contributed to writing the manuscript.

Competing Interests Statement

The authors declare no competing interests.

References

1. Tymm, C., Zhou, J., Tadimety, A., Burklund, A. & Zhang, J. X. Scalable COVID-19 detection enabled by lab-on-chip biosensors. *Cellular and Molecular Bioengineering* **13**, 313–329 (2020).
2. Yager, P., Domingo, G. J. & Gerdes, J. Point-of-care diagnostics for global health. *Annual review of biomedical engineering* **10** (2008).
3. Peeling, R. & Mabey, D. Point-of-care tests for diagnosing infections in the developing world. *Clinical microbiology and infection* **16**, 1062–1069 (2010).
4. Chan, C. P. Y. *et al.* Evidence-based point-of-care diagnostics: current status and emerging technologies. *Annual review of analytical chemistry* **6**, 191–211 (2013).
5. Chen, H., Liu, K., Li, Z. & Wang, P. Point of care testing for infectious diseases. *Clinica Chimica Acta* **493**, 138–147 (2019).
6. Burgess, D. C. H., Wasserman, J. & Dahl, C. A. Global health diagnostics. *Nature* **444**, 1–2 (2006).
7. Han, K., Yoon, Y.-J., Shin, Y. & Park, M. K. Self-powered switch-controlled nucleic acid extraction system. *Lab on a Chip* **16**, 132–141 (2016).
8. Chua, A., Yean, C. Y., Ravichandran, M., Lim, B. & Lalitha, P. A rapid DNA biosensor for the molecular diagnosis of infectious disease. *Biosensors and Bioelectronics* **26**, 3825–3831 (2011).
9. Ngom, B., Guo, Y., Wang, X. & Bi, D. Development and application of lateral flow test strip technology for detection of infectious agents and chemical contaminants: a review. *Analytical and bioanalytical*

chemistry **397**, 1113–1135 (2010).

10. Posthuma-Trumpie, G. A., Korf, J. & van Amerongen, A. Lateral flow (immuno) assay: its strengths, weaknesses, opportunities and threats. A literature survey. *Analytical and bioanalytical chemistry* **393**, 569–582 (2009).
11. Rastkari, N. & Ahmadkhaniha, R. Magnetic solid-phase extraction based on magnetic multi-walled carbon nanotubes for the determination of phthalate monoesters in urine samples. *Journal of chromatography A* **1286**, 22–28 (2013).
12. Zhou, Y. *et al.* Comparison of kidney injury molecule-1 and other nephrotoxicity biomarkers in urine and kidney following acute exposure to gentamicin, mercury, and chromium. *Toxicological sciences* **101**, 159–170 (2008).
13. Soler-García, Á. A., Johnson, D., Hathout, Y. & Ray, P. E. Iron-Related Proteins: Candidate Urine Biomarkers in Childhood HIV–Associated Renal Diseases. *Clinical Journal of the American Society of Nephrology* **4**, 763–771 (2009).
14. Sia, S. K. & Whitesides, G. M. Microfluidic devices fabricated in poly (dimethylsiloxane) for biological studies. *Electrophoresis* **24**, 3563–3576 (2003).
15. Heyries, K. A. *et al.* Microfluidic biochip for chemiluminescent detection of allergen-specific antibodies. *Biosensors and Bioelectronics* **23**, 1812–1818 (2008).
16. Kim, N., Chan, W. X., Ng, S. H., Yoon, Y.-J. & Allen, J. B. Understanding Interdependencies between Mechanical Velocity and Electrical Voltage in Electromagnetic Micromixers. *Micromachines* **11**, 636 (2020).
17. Kim, N., Chan, W. X., Ng, S. H. & Yoon, Y.-J. An acoustic micromixer using low-powered voice coil actuation. *Journal of Microelectromechanical Systems* **27**, 171–178 (2018).
18. Xu, L., Wang, A., Li, X. & Oh, K. W. Passive micropumping in microfluidics for point-of-care testing. *Biomicrofluidics* **14**, 031503 (2020).
19. Nayak, S. *et al.* Integrating user behavior with engineering design of point-of-care diagnostic devices: theoretical framework and empirical findings. *Lab on a Chip* **19**, 2241–2255 (2019).
20. Laser, D. J. & Santiago, J. G. A review of micropumps. *Journal of micromechanics and microengineering* **14**, R35 (2004).
21. Das, C. & Payne, F. Design and characterization of low power, low dead volume electrochemically-driven microvalve. *Sensors and Actuators A: Physical* **241**, 104–112 (2016).
22. Bußmann, A. B., Durasiewicz, C. P., Kibler, S. H. A. & Wald, C. K. Piezoelectric titanium based microfluidic pump and valves for implantable medical applications. *Sensors and Actuators A: Physical* **323**, 112649 (2021).
23. Gholizadeh, A. & Javanmard, M. Magnetically actuated microfluidic transistors: Miniaturized micro-valves using magnetorheological fluids integrated with elastomeric membranes. *Journal of Microelectromechanical Systems* **25**, 922–928 (2016).

24. Liu, J., Liu, X. & Li, S. in 2016 *IEEE International Conference on Aircraft Utility Systems (AUS).* 564-569 (IEEE).
25. Hirai, S. & Kato, K. in *2015 24th IEEE International Symposium on Robot and Human Interactive Communication (RO-MAN).* 652-657 (IEEE).
26. Yang, B., Wang, B. & Schomburg, W. K. A thermopneumatically actuated bistable microvalve. *Journal of Micromechanics and Microengineering* **20**, 095024 (2010).
27. Megnin, C. *et al.* Shape memory alloy based controllable multi-port microvalve. *Microsystem Technologies* **26**, 793–800 (2020).
28. Zhang, A.-L., Zhang, X.-Q., Hu, W.-Y. & Fu, X.-T. A shape memory alloy microvalve switching off by surface acoustic wave. *Ferroelectrics* **506**, 1–9 (2017).
29. Choi, J.-W. *et al.* An integrated microfluidic biochemical detection system for protein analysis with magnetic bead-based sampling capabilities. *Lab on a Chip* **2**, 27–30 (2002).
30. van der Wijngaart, W., Ask, H., Enoksson, P. & Stemme, G. A high-stroke, high-pressure electrostatic actuator for valve applications. *Sensors and Actuators A: Physical* **100**, 264–271 (2002).
31. Teymoori, M. M. & Abbaspour-Sani, E. Design and simulation of a novel electrostatic peristaltic micromachined pump for drug delivery applications. *Sensors and Actuators A: Physical* **117**, 222–229 (2005).
32. Zimmermann, M., Schmid, H., Hunziker, P. & Delamarche, E. Capillary pumps for autonomous capillary systems. *Lab on a Chip* **7**, 119–125 (2007).
33. Martinez, A. W., Phillips, S. T. & Whitesides, G. M. Three-dimensional microfluidic devices fabricated in layered paper and tape. *Proceedings of the National Academy of Sciences* **105**, 19606-19611 (2008).
34. Glynou, K., Ioannou, P. C., Christopoulos, T. K. & Syriopoulou, V. Oligonucleotide-functionalized gold nanoparticles as probes in a dry-reagent strip biosensor for DNA analysis by hybridization. *Analytical Chemistry* **75**, 4155–4160 (2003).
35. Fu, Y. *et al.* A microfluidic chip based on surfactant-doped polydimethylsiloxane (PDMS) in a sandwich configuration for low-cost and robust digital PCR. *Sensors and Actuators B: Chemical* **245**, 414–422 (2017).
36. Salman, A., Carney, H., Bateson, S. & Ali, Z. Shunting microfluidic PCR device for rapid bacterial detection. *Talanta* **207**, 120303 (2020).
37. Song, Q. *et al.* Point-of-care testing detection methods for COVID-19. *Lab on a Chip* (2021).
38. Yang, Y., Chen, Y., Tang, H., Zong, N. & Jiang, X. Microfluidics for biomedical analysis. *Small methods* **4**, 1900451 (2020).
39. Gill, P. & Ghaemi, A. Nucleic acid isothermal amplification technologies—a review. *Nucleosides, Nucleotides and Nucleic Acids* **27**, 224–243 (2008).
40. Hartman, M. R. *et al.* Point-of-care nucleic acid detection using nanotechnology. *Nanoscale* **5**, 10141–10154 (2013).

41. Zhang, Y. & Ozdemir, P. Microfluidic DNA amplification—A review. *Analytica chimica acta* **638**, 115–125 (2009).
42. Ahmad, F. & Hashsham, S. A. Miniaturized nucleic acid amplification systems for rapid and point-of-care diagnostics: a review. *Analytica chimica acta* **733**, 1–15 (2012).
43. Kim, J. & Easley, C. J. Isothermal DNA amplification in bioanalysis: strategies and applications. *Bioanalysis* **3**, 227–239 (2011).
44. Niemz, A., Ferguson, T. M. & Boyle, D. S. Point-of-care nucleic acid testing for infectious diseases. *Trends in biotechnology* **29**, 240–250 (2011).
45. Li, J., Macdonald, J. & von Stetten, F. a comprehensive summary of a decade development of the recombinase polymerase amplification. *Analyst* **144**, 31–67 (2018).
46. Magro, L. *et al.* based RNA detection and multiplexed analysis for Ebola virus diagnostics. *Scientific reports* **7**, 1–9 (2017).
47. Liu, C., Mauk, M. G., Hart, R., Qiu, X. & Bau, H. H. A self-heating cartridge for molecular diagnostics. *Lab on a Chip* **11**, 2686–2692 (2011).
48. Huang, S. *et al.* Low cost extraction and isothermal amplification of DNA for infectious diarrhea diagnosis. *PLoS One* **8**, e60059 (2013).
49. Shin, Y., Perera, A. P., Wong, C. C. & Park, M. K. Solid phase nucleic acid extraction technique in a microfluidic chip using a novel non-chaotropic agent: dimethyl adipimidate. *Lab on a Chip* **14**, 359–368 (2014).

Figures

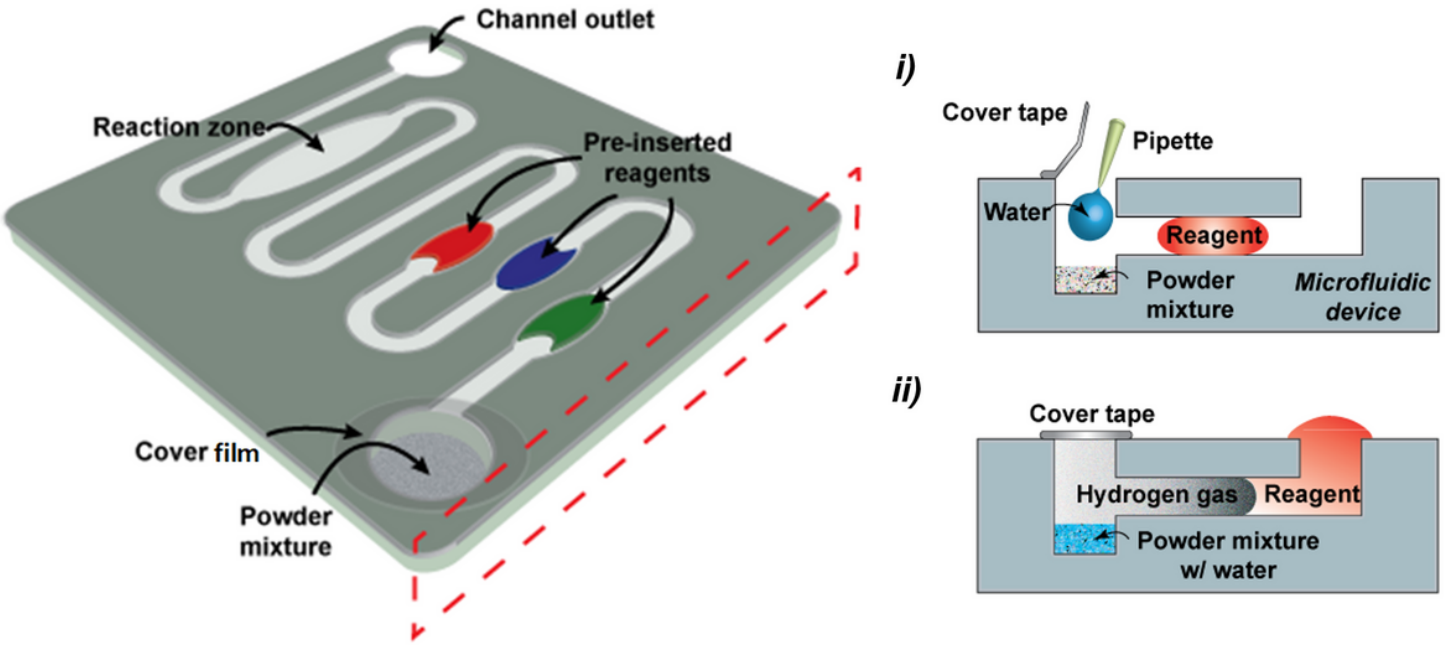

Figure 1

Schematic diagram of working principle for hydration reaction-based powerless actuator; i) applying water & attaching cover film and ii) producing hydrogen gas by hydration reaction & pushing reagent and basic design concept non-instrumented gas-driven microfluidic system. The formation of hydrogen gas from the powerless actuator is located in a microchannel inlet by applying water and covering the inlet hole. Sequential injection of pre-inserted reagents (red-blue-green) with air spacers between reagents through reaction zone to the microchannel outlet. Occurring reactions of reagents in the reaction zone according to the injection sequence.

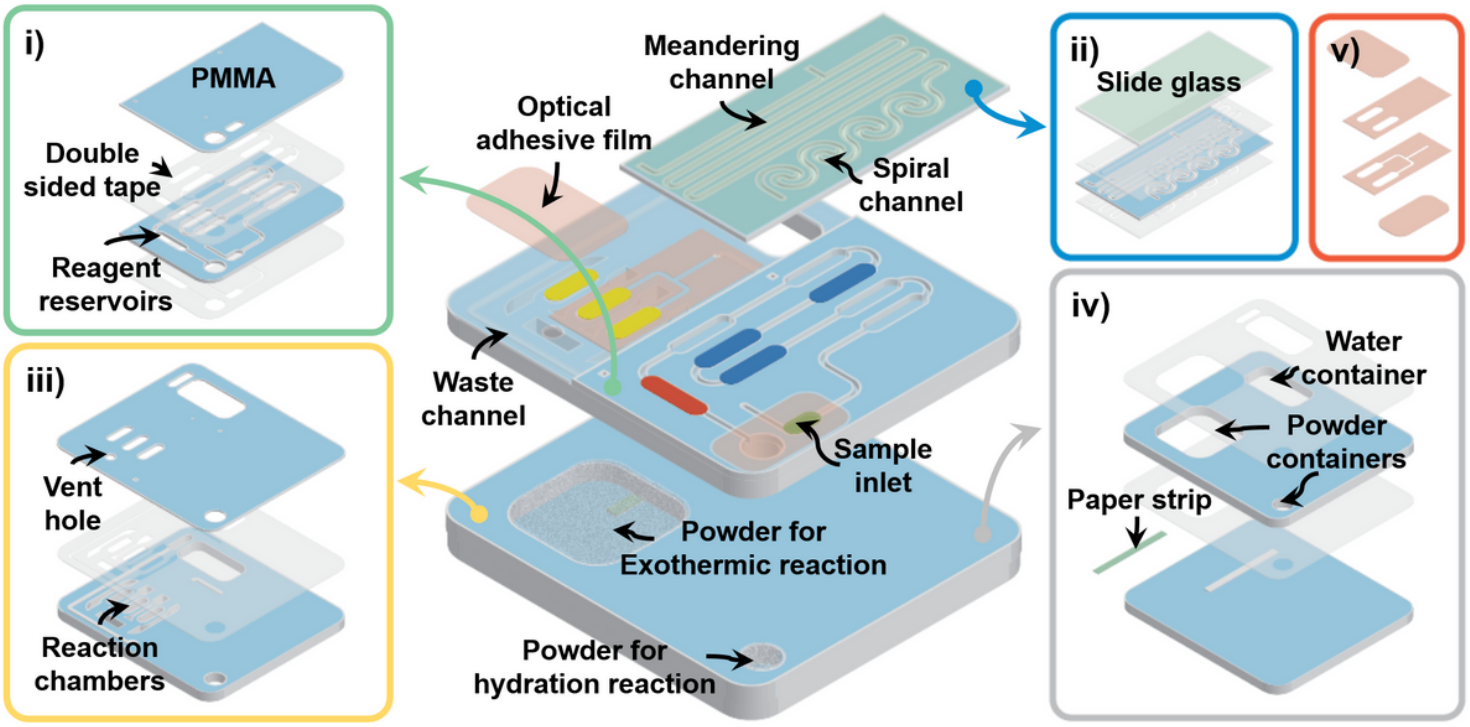

Figure 2

Schematic structural diagram of a disposable DNA analysis chip with a powerless actuator; i) reagent reservoir component, ii) DNA extraction component, iii) DNA amplification & detection component, and iv) water & powder container component. Fabrication of all components by cutting/engraving PMMA sheets and double-sided tapes using a CO_2 laser machine and assembly process of components performed with double-sided tapes. v) Cover films, bridge channels made by cutting optical adhesive films.

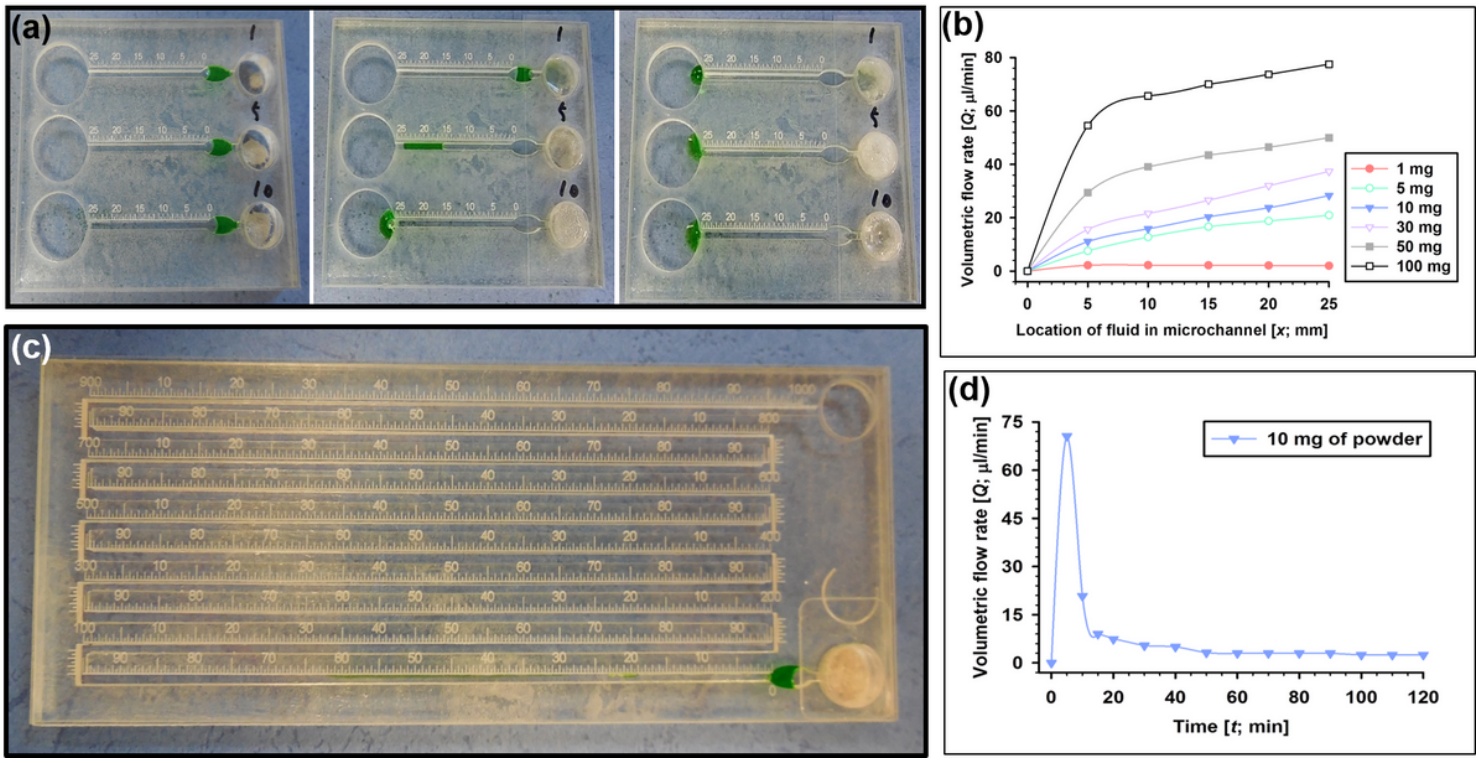

Figure 3

Images of; (a) three straight microchannels with 1 × 1 × 25 mm^3 volume for the flow rate measurement of formed gas by hydration reaction across the time measured and (c) along microchannel with 1 × 1 × 1000 mm^3 volume for the determination of flow rate uniformity and the duration of hydration reaction. Graphs of gas flow rate changes; (b) along the microchannel with different amounts of the powder with the kit shown in (a) and (d) over time with 10 mg of the powder with the kit shown in (c).

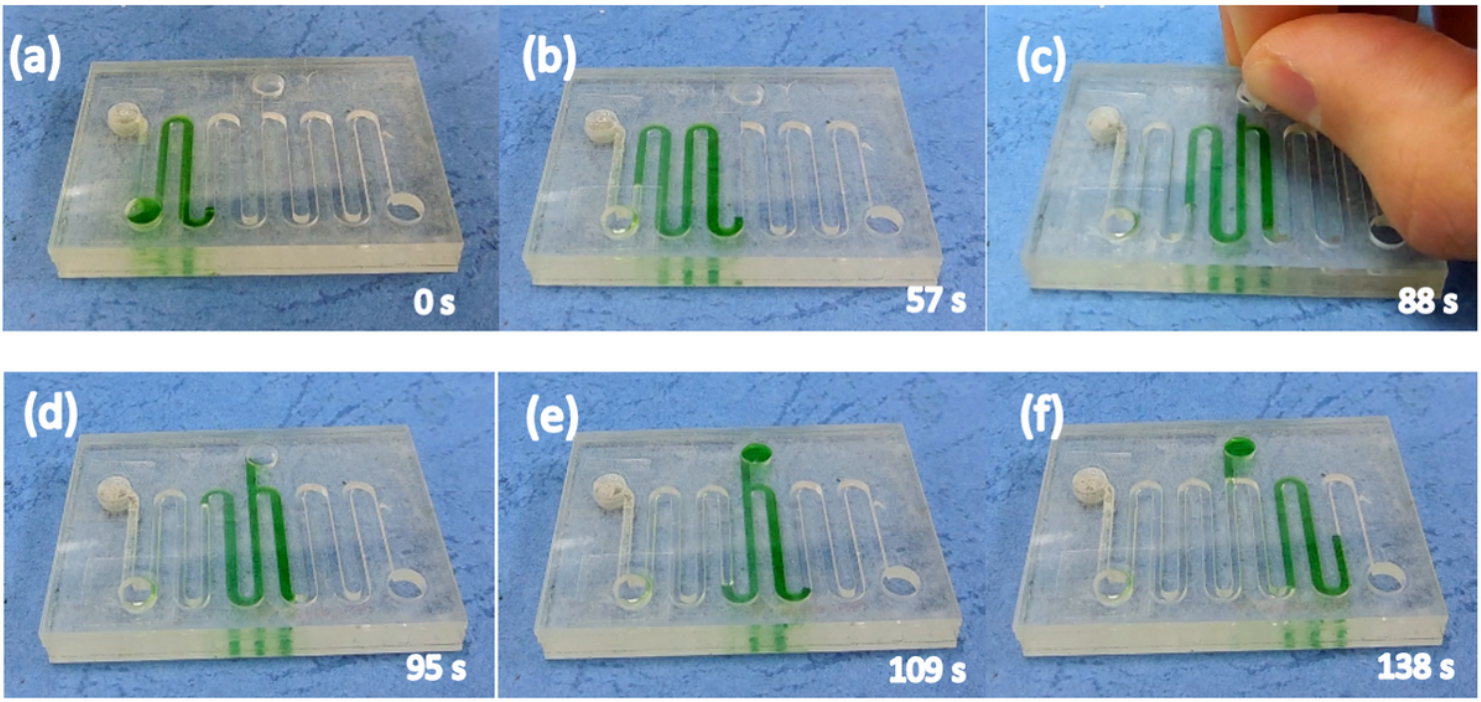

Figure 4

Images of; a long channel with a hydration reaction chamber on the top left, a waste chamber on the bottom right and a junction to the middle top reaction chamber. (a) Hydration reaction started and (b) pushed the eluted DNA solution (green) towards the junction. (c) The flim cover on the reaction chamber is removed after the eluted DNA solution passed slightly to replicate some operation error. The eluted DNA solution (d) travels to and (e) fills the reaction chamber. (f) When the chamber is filled the extra solution flows to the waste chamber without overflowing the reaction chamber.

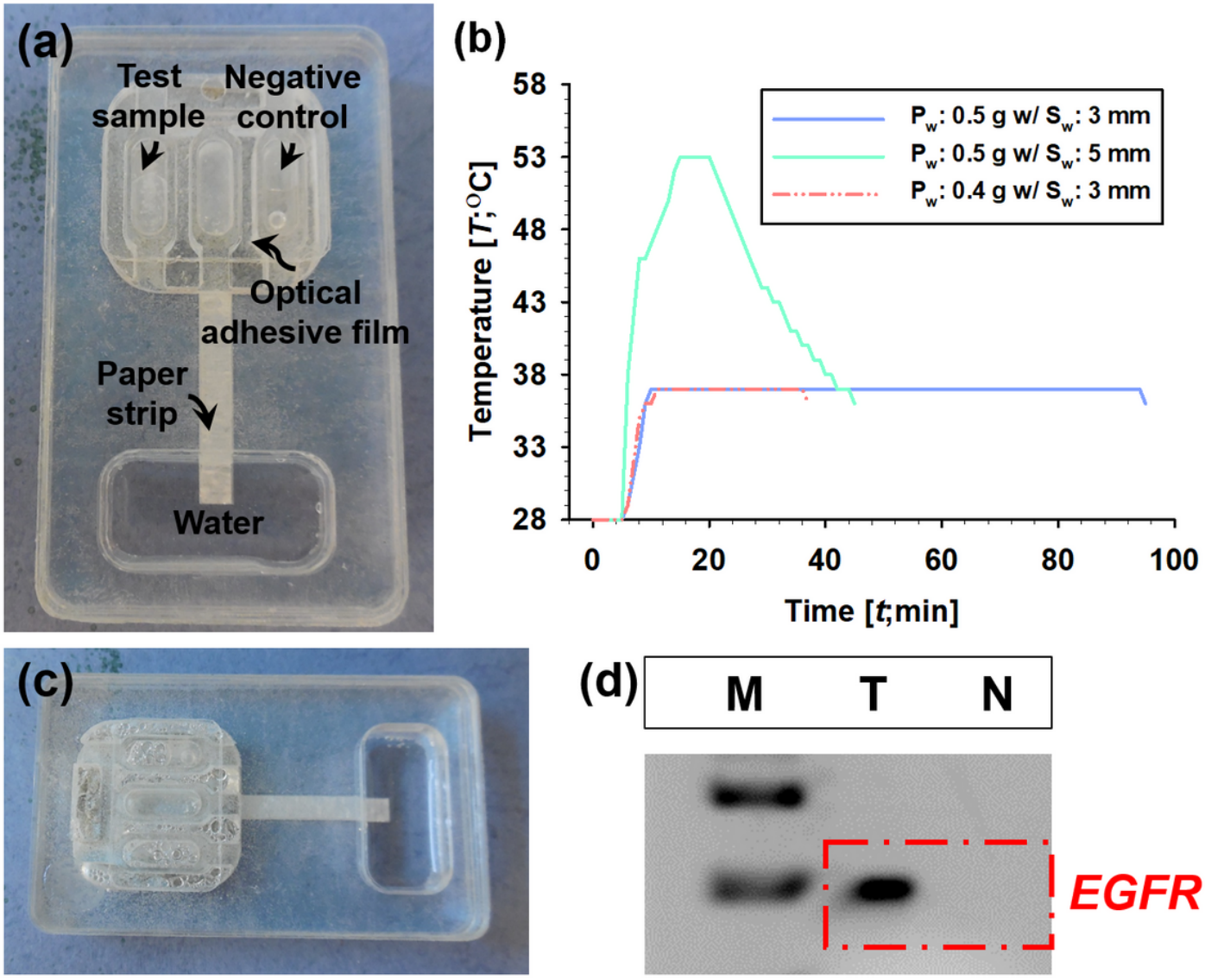

Figure 5

(a) Image of structure of the non-instrumented RPA device. Adding a test sample into the left reaction reservoir and a solution for negative control into the right reaction reservoir and attaching an optical adhesive film onto reaction chambers. (b) A graph of temperature variation plot with time using different combinations of exothermic reactive powder amounts (0.5 g and 0.4 g) and paper strip widths (3 mm and 5 mm). Initiate exothermic reactive powder by wicking water to the powder container 5 min after applying

water to a water reservoir. 0.5 g amount of the powder and 3 mm width of the paper strip met the required temperature and time for the RPA of DNA. (c) Image of the RPA device with decided condition captured during the RPA. (d) Image of cropped gel electropherogram result indicating DNA ladder (M), amplified test sample (T) and negative control (N); full-length gel electropherogram is presented in Figure S1.

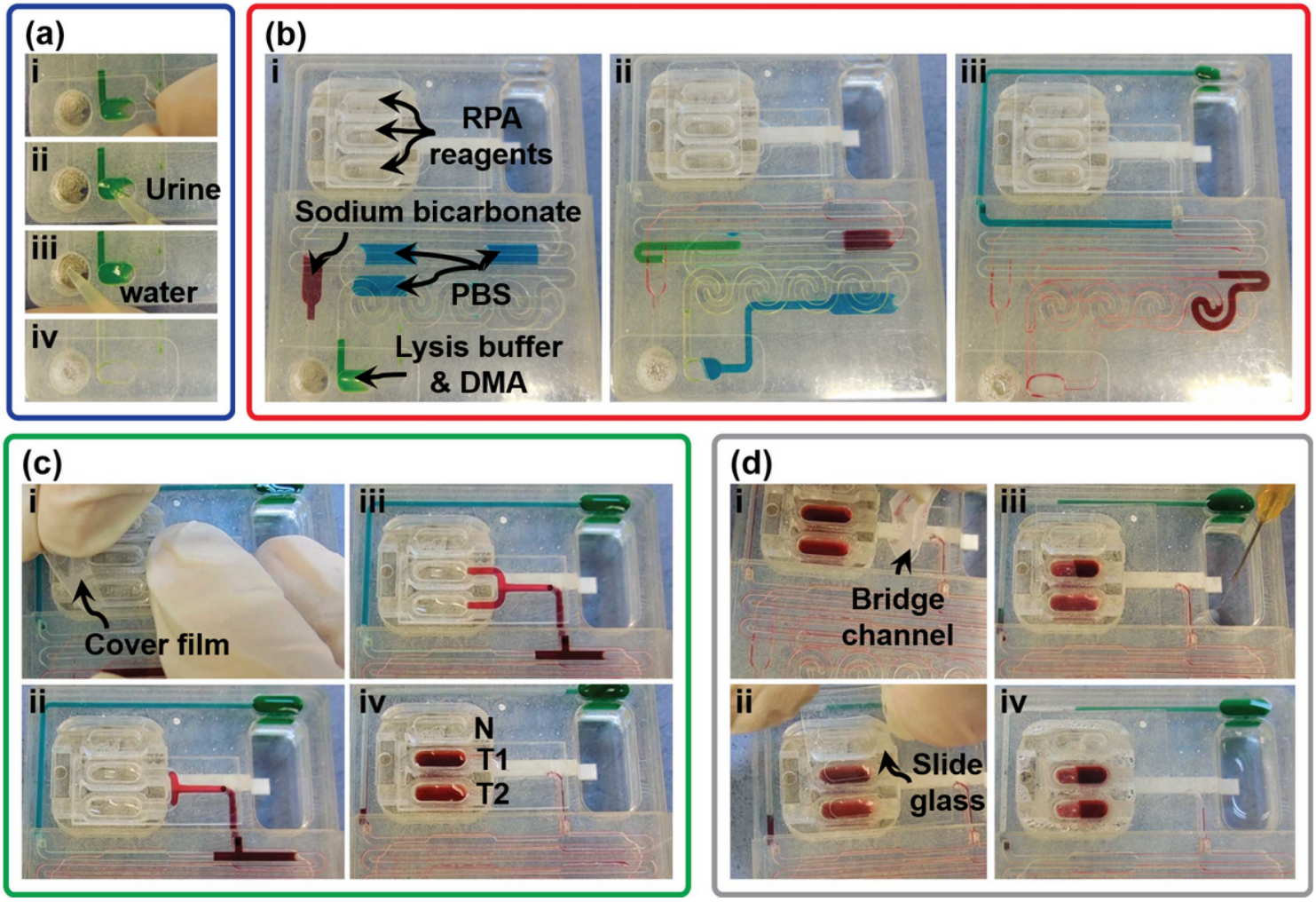

Figure 6

Images of analysis process of DNA from urine sample using the disposable DNA analysis chip with a powerless actuator; (a-i) detaching an optical adhesive film from the inlets of hydration reactive power container and test sample reservoir, (a-ii) adding urine sample to the reservoir, (a-iii) applying water to the powder container and (a-iv) attaching new adhesive film to initiate the hydration reaction based powerless actuator, (b-i) initial condition of the system, (b-ii) starting sequential injection and reaction, (b-iii) flowing the wastes out (lysis buffer & DMA & urine sample and PBS), (c-i) opening another outlet by detaching cover film from reaction chambers, (c-ii) changing flow direction of eluted DNA solution toward reaction chambers, (c-iii) separating the solution evenly to two reaction chambers, (c-iv) mixing the solutions with RPA reagents, (d-i) detaching bridge channel to isolate the reaction chambers, (d-ii) attaching slide glass with double-sided tape onto reaction chambers, (d-iii) adding water to the water container and (d-iv) incubating test samples for 35 min.

Supplementary Files

This is a list of supplementary files associated with this preprint. Click to download.

- Supplementaryinformation.docx